



HAL
open science

Nitrogen metastable ($N_2(A^3 \Sigma_u^+)$) in a cold argon atmospheric pressure plasma jet: Shielding and gas composition

Sylvain Iseni, Peter J. Bruggeman, Klaus-Dieter Weltmann, Stephan Reuter

► **To cite this version:**

Sylvain Iseni, Peter J. Bruggeman, Klaus-Dieter Weltmann, Stephan Reuter. Nitrogen metastable ($N_2(A^3 \Sigma_u^+)$) in a cold argon atmospheric pressure plasma jet: Shielding and gas composition. Applied Physics Letters, 2016, 108 (18), pp.184101-184101. 10.1063/1.4948535 . hal-02270227

HAL Id: hal-02270227

<https://hal.science/hal-02270227>

Submitted on 21 May 2021

HAL is a multi-disciplinary open access archive for the deposit and dissemination of scientific research documents, whether they are published or not. The documents may come from teaching and research institutions in France or abroad, or from public or private research centers.

L'archive ouverte pluridisciplinaire **HAL**, est destinée au dépôt et à la diffusion de documents scientifiques de niveau recherche, publiés ou non, émanant des établissements d'enseignement et de recherche français ou étrangers, des laboratoires publics ou privés.

Nitrogen metastable ($N_2(A^3\Sigma_u^+)$) in a cold argon atmospheric pressure plasma jet: shielding and gas composition

Sylvain Iseni,^{1,2, a)} Peter J. Bruggeman,³ Klaus-Dieter Weltmann,² and Stephan Reuter^{1,2}

¹⁾Center for Innovation Competence plasmatis, 17489 Greifswald, Germany.

²⁾Leibniz Institute for Plasma Science and Technology (INP), 17489 Greifswald, Germany.

³⁾Department of Mechanical Engineering, University of Minnesota, 111 Church Street SE, Minneapolis, MN 55455, USA.

(Dated: May 21, 2021)

$N_2(A^3\Sigma_u^+)$ metastable species are detected and measured in a non-equilibrium atmospheric pressure plasma jet by laser induced fluorescence (LIF). A shielding device is used to change the ambient conditions additionally to the feeding gas composition. Varying the amount of N_2 and air admixed to the feeding gas as well as changing the shielding gas from N_2 to air reveals that the highest $N_2(A^3\Sigma_u^+)$ is achieved in the case of air admixtures in spite of the enhanced collisional quenching due the presence of O_2 . The reasons for these observations are discussed in detail.

This article may be downloaded for personal use only. Any other use requires prior permission of the author and AIP Publishing. This article appeared in S. Iseni, P.J. Bruggeman, K.-D. Weltmann, and S. Reuter, Appl. Phys. Lett. 108, 184101 (2016) and may be found at <https://doi.org/10.1063/1.4948535>.

Keywords: nitrogen metastable; laser-induced fluorescence; argon; atmospheric pressure plasma jet; plasma medicine.

The interest in cold atmospheric pressure plasma jets (APP jets) has been growing continuously over the last decade, particularly in view of therapeutic applications¹. APP jets are often obtained by noble gases –mostly helium (He), argon (Ar)– flowing through a capillary tube. This yields a low temperature reactive plasma plume expanding into the surrounding air². Recent publications reporting the interaction of APP jets with biological tissues³ evidence the real potential of such plasma sources to trigger beneficial biological responses. The impact of plasma on cells has been largely attributed to the presence of reactive oxygen and nitrogen species⁴ (RONS) resulting from the non-equilibrium plasma chemistry reacting with ambient humid air⁵. Among these RONS, nitric-oxide (NO) is of significant importance due to its high reactivity and key role in biological pathways. NO plays a key role in cell signaling and vascularization⁴. The production of such RONS by cold Ar APP jets results from a complex non-equilibrium chemistry involving several reaction pathways⁶. Van Gaens *et al.*^{7,8} have identified that NO production is not governed by the Zel'dovich reactions –as it is the case at elevated gas temperatures for combustion conditions– but rather via electronically excited $N_2(A^3\Sigma_u^+)$ –metastable state– reacting with atomic oxygen (O). As $N_2(A^3\Sigma_u^+)$ is a precursor species for the production of NO⁷, the obtained results in this manuscript are valuable to gain a better understanding of the NO production in cold plasma jets.

Several groups have already studied atomic He^{9–11} and Ar⁹ metastables in APP jets. With a strong focus on He

O_2 and Ar- O_2 mixtures, these metastables are important precursors for RONS formation. However metastable molecules including the $N_2(A^3\Sigma_u^+)$ have not been investigated in cold APP jets.

Investigations of $N_2(A^3\Sigma_u^+)$ in atmospheric pressure discharges have been performed in corona¹², streamer¹³ and dielectric barrier discharge (DBD)¹⁴. The direct quantitative measurement of $N_2(A^3\Sigma_u^+)$ remains challenging. Several approaches are reported in literature involving different diagnostic techniques such as optical emission spectroscopy¹⁵ (OES), cavity ring-down spectroscopy¹⁶ (CRDS) and laser-induced fluorescence^{13,17} (LIF). Common challenges for those diagnostics are the absolute calibration and the often weak fluorescence or absorption signals. Optical-optical double resonance LIF (OODR-LIF) was introduced by Dilecce *et al.*¹⁴ to enhance the weak fluorescence signal but is a complex technique to implement.

In this letter, we report on the detection and measurement of the relative density of $N_2(A^3\Sigma_u^+)$ in the plasma plume of a radio-frequency driven Ar APP jet with a coaxial geometry: the *kinpen*¹⁸. The plasma dissipates a power ranging between 0.8 W to 2.2 W and the gas temperature is less than 500 K¹⁹. The source is operated at the flow rate of 1.0 standard liter per minute (slm). The feeding gas is Ar with small admixtures (up to 1%) of N_2 and air. The 1.0 slm flow rate is chosen to ensure a laminar gas flow²⁰ and to prevent excessive mixing of the effluent gas containing RONS with the surrounding gas¹⁹. Additionally, a custom-made nozzle covers the device head and generates –via an external gas flow– a gas shielding enveloping the plasma plume^{21,22}. This controls the gas species surrounding and diffusing into the plasma effluent.

^{a)}Corresponding author: sylvain.iseni@univ-orleans.fr

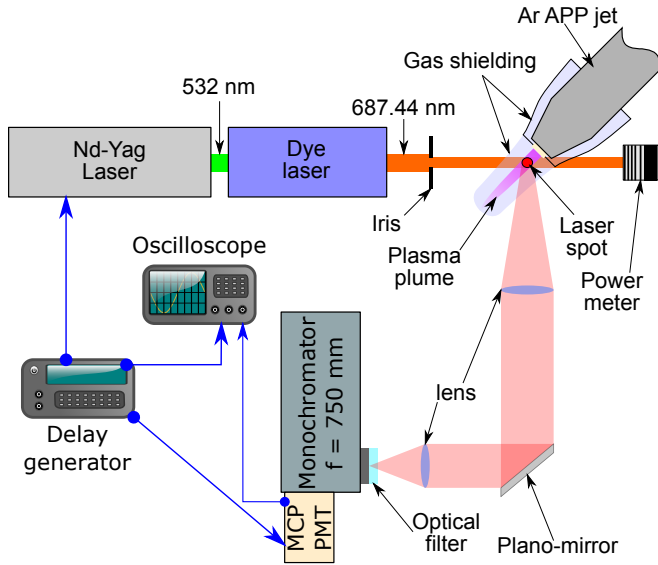


Figure 1. Schematic of the experimental setup used for the measurement of $N_2(A^3\Sigma_u^+)$ in a cold Ar APP jet with shielding gas.

In this work, LIF is used for its good spatial and temporal resolution. A scheme of the experimental setup is shown in figure 1. A dye laser (Sirah Lasertechnik, Cobra-Stretch) with pyridine 1 is pumped by a frequency doubled Nd:YAG laser (Spectra-Physics, Quanta-Ray Pro-230). The laser has a pulse a duration of ~ 11.9 ns (FWHM) and operates at 10 Hz. The dye laser is tuned to 687.44 nm (with a linewidth of $\Delta\lambda=2.2$ pm FWHM) to pump the lower rotational levels ($J \leq 4$) of the P_{11} and Q_{12} branch from the transition $N_2(B^3\Pi_g, v = 3) \leftarrow N_2(A^3\Sigma_u^+, v = 0)$ ¹⁴. The laser beam is cropped with an iris to produce a 2.0 mm diameter spot to probe a plasma plume volume 2.0 mm away from the capillary exit if not stated otherwise. The laser irradiance (I_L) is (60.0 ± 1.6) mJ/cm². We have checked that the LIF intensity scales linearly with the laser energy at this irradiance. The LIF signal (S_{LIF}) of the transition $N_2(B^3\Pi_g, v = 3) \rightarrow N_2(A^3\Sigma_u^+, v = 1)$ is imaged with a lens on the slit of a monochromator (Andor Technology ltd., Shamrock 750, 1200 grooves ruled grating Blazed at 500 nm) fine-tuned on 762 nm. The later is also equipped with a bandpass filter (cw:760 nm, FWHM:10 nm) to block the stray light. The detection range of this system is 9.1 nm allowing to record the entire vibrational band. The signal is recorded by a multi-channel plate photo multiplier (MCP-PMT, Hamamatsu, R5916U-51) read out by an oscilloscope (Tektronix, DPO 70000, 8 GHz bandwidth).

The LIF technique is applied in this work under the following assumptions:

- The laser energy is low enough to excite a small fraction of $N_2(A^3\Sigma_u^+, v = 0)$ so that its population is considered constant and the population of the excited state is much smaller than the ground

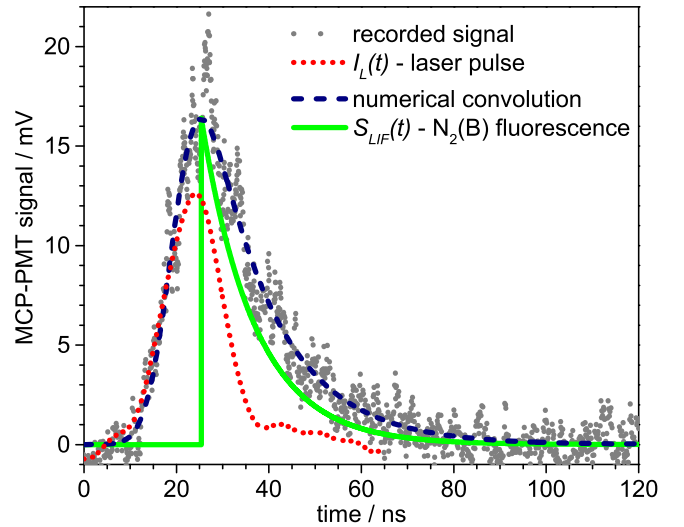


Figure 2. Time resolved LIF signal and Rayleigh signal in air as recorded by the MCP-PMT. The fluorescence curve of $N_2(B^3\Pi_g)$ is calculated from the fit of the LIF signal by a convolution of the laser pulse with an exponential decay ($\tau=11.4$ ns). The data is recorded for Ar + 1.0 % air and N_2 as a shielding gas.

state. Thus, the effect of stimulated emission can be neglected.

- The emission coefficients and quenching rates are assumed to be identical for all rotational states of $N_2(B^3\Pi_g, v = 3)$ and the rotational energy transfer is fast compared with the fluorescence time scale.
- Both rotational levels of the ground state and the metastable state $N_2(A^3\Sigma_u^+)$ are in equilibrium with the gas temperature and can be described with a Boltzmann distribution.

This formalism was also used by van Gessel *et. al.* for the diagnostic of NO under similar conditions²³. The density of $N_2(A^3\Sigma_u^+)$, $n_{N_2(A)}$, is in this case proportional to the ratio of the fluorescence intensity and is the effective fluorescence lifetime,

$$n_{N_2(A)} \propto \frac{S_{LIF}}{\tau \cdot I_L}, \quad (1)$$

where $\tau = (A_B + Q)^{-1}$ the fluorescence lifetime. A_B (in 1/s) is the spontaneous emission rate of the $v = 3$ level (2.30×10^6 /s)²⁴ and $Q = \sum_i q_i \cdot n_i$ (1/s) the quenching rate with q_i (cm³/s) the quenching rate coefficient and n_i (1/cm³) the density of the quencher i .

Figure 2 presents a typical time evolution of the fluorescence signal recorded by the MCP-PMT after an averaged acquisition of 10^4 shots. Compared with the laser excitation pulse $I_L(t)$, the signal has a clear asymmetric evolution and results from the convolution of $I_L(t)$ with an exponential decay. Since the jitter of the laser is less than 0.5 ns, the time instrument response function

Table I. Measured values of τ and Q for different combinations of feeding gas admixtures and shielding gas.

Admix.	Shield.	$\tau / 10^{-9} \text{ s}$	$Q / 10^7 / \text{s}$
N ₂	N ₂	19.7 ± 1.5	5.1 ± 0.4
N ₂	air	8.6 ± 0.6	11.6 ± 0.8
air	N ₂	10.8 ± 1.9	9.4 ± 1.6
air	air	6.1 ± 0.9	16.4 ± 2.4
^a N ₂	air	8.5 ± 0.6	11.7 ± 0.8

^a Value obtained at 5.0 mm from the capillary.

Table II. Quenching rate coefficients (q_i) of N₂(A³Σ_u⁺) and N₂(B³Π_g) for different gases.

Quencher	Rate / 10 ⁻¹¹ cm ³ /s			
	N ₂ (A ³ Σ _u ⁺)	ref.	N ₂ (B ³ Π _g)	ref.
Ar+ 0.3% N ₂	-		>1	²⁵
N ₂	10 ⁻⁹	²⁶	3 ± 0.2	^{27,28}
O ₂	0.50 ± 0.03	²⁹	20 ± 0.5	²⁸
N ₂ (A ³ Σ _u ⁺)	19 ± 0.5	²⁷	-	
NO	8.0 ± 1.5	²⁹	-	
O	3.1 ± 0.5	³⁰	-	

of our MCP-PMT is 85 ps and the time constant of the measuring circuit with 50 Ω load is 1.3 ns, one can safely assume that both signals presented in figure 2 are not significantly altered by the detection system. A numerical convolution between $I_L(t)$ and an exponential function, $A_{LIF} \cdot \exp(-\frac{t}{\tau})$, is computed and optimized with a Levenberg-Marquardt algorithm to obtain the best fit of the recorded signal. The amplitude, A_{LIF} and the decay time τ are the fitting parameters. An example is shown in figure 2. $S_{LIF} = A_{LIF} \cdot \tau$ is the integration of the fluorescence signal. This provides the necessary input for equation 1 to calculate $n_{N_2(A)}$.

We measured N₂(A³Σ_u⁺) relative densities using both N₂ and air as admixture and shielding gas. Table I introduces the measured values of the fluorescence decay time and the deduced quenching rate (coefficient) for different gas admixture/gas shielding parameter sets. The case with N₂ admixtures and N₂ shielding has a longer radiative lifetime of the N₂(B³Π_g) state, while an admixture of air in the plasma plume, or air gas shielding reduces the fluorescence lifetime by a factor 3. This is explained by the O₂ fraction in the buffer gas. O₂ quenches the N₂(B³Π_g) state much more effectively compared with N₂ and Ar. Table II reports quenching rate coefficients of the N₂(B³Π_g) state for the main gases used in this work. In the cases where air and N₂ are simultaneously used as admixture and/or shielding gas, quenching rates are similar. The influence of the gas temperature on the quenching rate is estimated to be about 15% between positions 1.5 mm and 5.0 mm due to a temperature difference of ~50 K¹⁹.

Relative densities of N₂(A³Σ_u⁺) as a function of air or N₂ admixture are presented in figure 3 for air and N₂

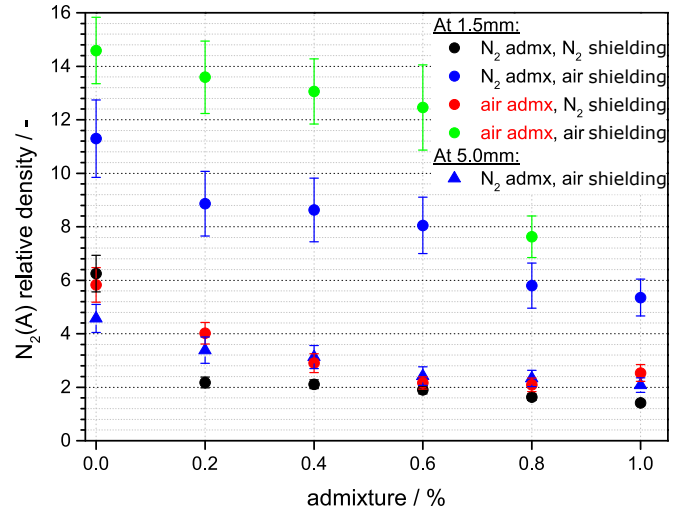


Figure 3. N₂(A³Σ_u⁺) relative densities versus feeding gas admixture fractions for different types of gas shielding. The measurements are space averaged over the section of the plasma plume (2 mm) and time averaged over 10⁴ laser shots.

shielding. $n_{N_2(A)}$ can vary by a factor 7 depending on the type of admixture ranging from 0% to 1% and the air or N₂ shielding gas diffusing in the plasma plume. As a result, an increase of molecular gas fraction up to 1.0% induces a decrease in metastable density exceeding a factor 2.5 for all conditions. It is not excluded that the molecular admixtures affect the deposited power in the plasma. This may result in a density drop such as observed between 0.6% and 0.8%. This was already observed by Verreycken *et. al.*³¹ in the case of OH production. Densities obtained by chemical kinetics model of this discharge⁸ follow the same trend and are in good agreement with the case of N₂ admixtures and air shielding presented in figure 3. Variations of $n_{N_2(A)}$ without admixture of air or N₂ result from the fact that experimentally, pure Ar conditions are challenging to achieve due to inherent impurities in the feeding gas. Interestingly, a significant increase of $n_{N_2(A)}$ is observed when the plasma plume is surrounded by air while no molecular admixture is supplied. This means that the diffusion of air into the plasma plume influences the plasma chemistry enhancing the generation of N₂(A³Σ_u⁺). In addition, the presence of O₂ while admixing air was expected to negatively impact $n_{N_2(A)}$ since O₂ is an efficient quencher of N₂(A³Σ_u⁺) (*cf.* table II).

Recently, van Gessel *et. al.*³² published an experimental study of electron properties of an Ar APP jet similar to the plasma device used in this work. The authors report similar electron temperatures (T_e) with admixtures of N₂ and air in the Ar jet while the electron density (n_e) is higher for the air admixture than N₂ admixture case. As in this discharge the formation mechanism of N₂(A³Σ_u⁺) is mostly driven by direct electron impact⁸, a strong correlation between $n_{N_2(A)}$ and n_e is expected. A similar dependence was notified by the same group³³

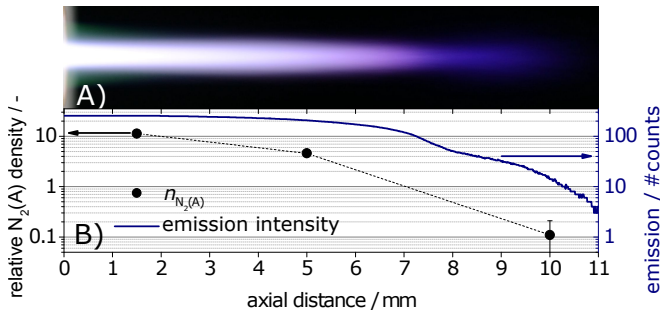


Figure 4. A) Image of the visual plasma emission (exp. time: 0.25 s). B) Axial density distribution of $N_2(A^3\Sigma_u^+)$ and light emission intensity of the plasma plume for the case of 0.1% N_2 admixture to the feeding gas and air as the shielding.

with the observation of $NO(A)$ emission resulting from an excitation of $NO(X)$ by $N_2(A^3\Sigma_u^+)$. The $NO(A)$ emission intensity gives a relative estimation of $n_{N_2(A)}$ and correlates with the measured n_e during one modulation cycle³². Moreover, higher n_e in the presence of air may also compensate the quenching of $N_2(A^3\Sigma_u^+)$ by O_2 .

According to figure 3, the nature of the gas shielding has a larger influence on $n_{N_2(A)}$ than the reduction of O_2 in the feed gas while admixing air. Surprisingly, $n_{N_2(A)}$ is higher when the plasma plume is surrounded by air with air admixture (●) than in conditions with air substituted by N_2 (●). One infers from this result that a reduction of O_2 in the shielding gas is not conducive to the production of $N_2(A^3\Sigma_u^+)$. Schmidt-Bleker *et al.* published the results of a combined theoretical and experimental work and suggest an explanation for the enhancement of the discharge intensity in the presence of O_2 in the shielding gas³⁴. The presence of electronegative molecules, such as O_2 , in the vicinity of the plasma plume is prone to form anions. Their lower mobility compared with electrons induces an additional electrostatic focusing mechanism³⁴ which confines the electric field parallel to the gas flow and leads to the generation of a more intense discharge. The case of air used as a feeding gas admixture and as shielding gas (●) may benefit from the combination of a higher n_e with the contribution of an electrostatic focusing mechanism. This results in the highest production of $N_2(A^3\Sigma_u^+)$ for this condition.

Figure 4 shows the axial evolution of $n_{N_2(A)}$. In view of the lifetime of $N_2(A^3\Sigma_u^+)$ which equals approximately 5 μ s (for Ar + 1% air), the $N_2(A^3\Sigma_u^+)$ is confined to the active plasma zone. Figure 4 even shows that the $N_2(A^3\Sigma_u^+)$ density is reduced by 2 orders of magnitude within the active plasma effluent. This is in agreement with prior numerical chemistry kinetic analysis⁸ on $N_2(A^3\Sigma_u^+)$ ranging from $10^{14}/\text{cm}^3$ to $10^{12}/\text{cm}^3$. Van Gessel *et al.* found similarly a strong correlation between the $NO(A)$ emission and the active plasma effluent.

In conclusion, $N_2(A^3\Sigma_u^+)$ relative densities have been measured by LIF in a low temperature Ar APP jet

(<500 K). The $N_2(A^3\Sigma_u^+)$ density strongly correlates with the discharge intensity and is confined to the active plasma zone. Interestingly, a reduction of O_2 in the feeding gas and surrounding gas is not prone to the production of $N_2(A^3\Sigma_u^+)$. The maximum production is achieved in the case of air that enhances the discharge intensity. This is explained by a higher n_e and electrostatic focusing mechanism for this condition. $N_2(A^3\Sigma_u^+)$ is an important intermediate specie responsible for the production of NO in many biomedical applications.

SI and SR would like to thank Prof. J. Meichsner and Dr. S. Nemschokmichal from the Institute of Physics, University of Greifswald, Germany, for the fruitful conversations and advise. This work was funded by the German Federal Ministry of Education and Research (Grant No 03Z2DN12). PJB acknowledges funding from the Department of Energy Plasma Science Center through the U.S. Department of Energy, Office of Fusion Energy Sciences (contract DE-SC0001939).

REFERENCES

- 1T. von Woedtke, S. Reuter, K. Masur, and K. D. Weltmann, *Physics Reports* **530**, 291 (2013).
- 2X. Lu, M. Laroussi, and V. Puech, *Plasma Sources Science and Technology* **21**, 034005 (2012).
- 3G. Collet, E. Robert, A. Lenoir, M. Vandamme, T. Darny, S. Dozias, C. Kieda, and J. M. Pouvlesle, *Plasma Sources Science Technology* **23**, 012005 (2014).
- 4D. B. Graves, *Journal of Physics D: Applied Physics* **45**, 263001 (2012).
- 5W. v. Gaens and A. Bogaerts, *Journal of Physics D: Applied Physics* **46**, 275201 (2013).
- 6W. v. Gaens and A. Bogaerts, *Plasma Sources Science and Technology* **23**, 035015 (2014).
- 7W. v. Gaens, P. J. Bruggeman, and A. Bogaerts, *New Journal of Physics* **16**, 063054 (2014).
- 8W. v. Gaens, S. Iseni, A. Schmidt-Bleker, K. D. Weltmann, S. Reuter, and A. Bogaerts, *New Journal of Physics* **17**, 033003 (2015).
- 9B. Niermann, M. Böke, N. Sadeghi, and J. Winter, *The European Physical Journal D* **60**, 489 (2010).
- 10K. Niemi, J. Waskoenig, N. Sadeghi, T. Gans, and D. O'Connell, *Plasma Sources Science and Technology* **20**, 055005 (2011).
- 11J. Winter, J. S. Sousa, N. Sadeghi, A. Schmidt-Bleker, S. Reuter, and V. Puech, *Plasma Sources Science and Technology* **24**, 025015 (2015).
- 12R. Ono and T. Oda, *Journal of Applied Physics* **97**, 013302 (2005).
- 13M. Šimek, *Plasma Sources Science and Technology* **12**, 421 (2003).
- 14G. Dilecce, P. F. Ambrico, and S. De Benedictis, *Plasma Sources Science Technology* **16**, 511 (2007).
- 15A. M. Pointu and G. D. Stancu, *Plasma Sources Science and Technology* **20**, 025005 (2011).
- 16G. D. Stancu, M. Janda, F. Kaddouri, D. A. Lacoste, and C. O. Laux, *The Journal of Physical Chemistry A* **114**, 201 (2010).
- 17S. Nemschokmichal and J. Meichsner, *Plasma Sources Science and Technology* **22**, 015005 (2013).
- 18K. D. Weltmann, E. Kindel, R. Brandenburg, C. Meyer, R. Busiahn, C. Wilke, and T. von Woedtke, *Contributions to Plasma Physics* **49**, 631 (2009).
- 19S. Iseni, S. Zhang, A. F. H. van Gessel, S. Hofmann, B. T. J. van

- Ham, S. Reuter, K. D. Weltmann, and P. J. Bruggeman, *New Journal of Physics* **16**, 123011 (2014).
- ²⁰S. Iseni, A. Schmidt-Bleker, J. Winter, K. D. Weltmann, and S. Reuter, *Journal of Physics D: Applied Physics* **47**, 152001 (2014).
- ²¹S. Reuter, J. Winter, A. Schmidt-Bleker, H. Tresp, M. U. Hammer, and K. D. Weltmann, *IEEE Transactions on Plasma Science* **40**, 2788 (2012).
- ²²S. Bekeschus, S. Iseni, S. Reuter, K. Masur, and K.-D. Weltmann, *IEEE Transactions on Plasma Science* **43**, 776 (2015).
- ²³A. F. H. van Gessel, B. Hrycak, M. Jasiński, J. Mizeraczyk, J. J. A. M. van der Mullen, and P. J. Bruggeman, *Journal of Physics D: Applied Physics* **46**, 095201 (2013).
- ²⁴L. G. Piper, K. W. Holtzclaw, B. D. Green, and W. A. M. Blumberg, *The Journal of Chemical Physics* **90**, 5337 (1989).
- ²⁵N. Sadeghi and D. W. Setser, *The Journal of Chemical Physics* **79**, 2710 (1983).
- ²⁶J. F. Noxon, *Journal of Chemical Physics* **36**, 926 (1962).
- ²⁷L. G. Piper, *The Journal of Chemical Physics* **88**, 6911 (1988).
- ²⁸L. G. Piper, *The Journal of Chemical Physics* **97**, 270 (1992).
- ²⁹J. Dreyer, D. Perner, and C. Roy, *The Journal of Chemical Physics* **61**, 3164 (1974).
- ³⁰L. Piper, G. Caledonia, and J. Kennealy, *The Journal of Chemical Physics* **75**, 2847 (1981).
- ³¹T. Verreycken, R. Mensink, R. van der Horst, N. Sadeghi, and P. J. Bruggeman, *Plasma Sources Sci. Technol.* **22**, 055014 (2013).
- ³²B. van Gessel, R. Brandenburg, and P. Bruggeman, *Applied Physics Letters* **103**, 064103 (2013).
- ³³A. Van Gessel, K. Alards, and P. Bruggeman, *Journal of Physics D: Applied Physics* **46**, 265202 (2013).
- ³⁴A. Schmidt-Bleker, S. A. Norberg, J. Winter, E. Johnsen, S. Reuter, K. D. Weltmann, and M. J. Kushner, *Plasma Sources Science and Technology* **24**, 035022 (2015).